

Waveform proportionality and Taylor's law in coupled Lorenz systems

Yuzuru Mitsui^{1,2,*} and Hiroshi Kori³

¹*Faculty of Design, Kyushu University, Shiobaru, Fukuoka, 815-8540, Japan*

²*Education and Research Center for Mathematical and Data Science,
Kyushu University, Motooka, Fukuoka, 819-0395, Japan*

³*Department of Complexity Science and Engineering,
The University of Tokyo, Kashiwa, Chiba 277-8561, Japan*

(Dated: July 7, 2025)

Taylor's law (TL), a power-law relationship between the mean and variance of a quantity, has been observed across diverse scientific disciplines. Despite its ubiquity, the underlying mechanisms responsible for TL are not yet fully elucidated. In particular, the frequent empirical observation of TL with an exponent 2 warrants further investigation. In a previous study [Phys. Rev. Lett. 134, 167202 (2025)], we hypothesized that synchronization contributes to the emergence of TL with an exponent 2. To validate this hypothesis, we employed coupled oscillator models, with each oscillator described by a distinct dynamical system: a food chain model, the Rössler system, the Brusselator, and the Lorenz system. Our analytical and numerical results demonstrated that strong coupling leads to a form of synchronization wherein time series become proportional to each other, consequently resulting in TL with an exponent 2. Here, we extend our previous findings for the coupled Lorenz system and provide detailed calculations. Our analytical and numerical results demonstrate that, under strong coupling, waveform proportionality and Taylor's law with an exponent 2 emerge not only in the original Lorenz system but also in the generalized and hyperchaotic Lorenz systems.

I. INTRODUCTION

Taylor's law (TL) [1, 2], also known as fluctuation scaling, quantifies a power-law relationship between the mean and variance of a variable. This law has been extensively observed across various fields, with its origins in ecology [3, 4]. TL is typically categorized into two types based on the method of calculating the mean and variance: temporal TL and spatial TL. Temporal TL utilizes the time average and variance of time series, whereas spatial TL employs the ensemble average and variance. Denoting the proportionality coefficient and exponent of temporal TL as α_t and β_t , respectively, and those of spatial TL as α_s and β_s , respectively, TL is expressed as

$$\log(\text{variance}) = \log \alpha_{t,s} + \beta_{t,s} \times \log(\text{mean}). \quad (1)$$

When the exponent takes values greater than one, this power-law relationship is often referred to as giant (number/density) fluctuations, a phenomenon extensively studied in the field of active matter physics [5–7]. Empirical data on population abundance in ecosystems frequently yield TL exponents close to 2 [8–10]. However, theoretical investigations have demonstrated that the TL exponent can take arbitrary real values [11–13], stimulating interest in understanding the mechanisms underlying the frequent emergence of TL with an exponent 2 [14]. In this context, we posited that synchronization underlies the emergence of TL with an exponent 2 [15], as several studies have indicated that stronger correlations between time series tend to drive the TL exponent towards 2 [9, 16, 17]. Intriguingly, when the correlation

becomes sufficiently strong such that the time series become proportional to each other, spatial TL with an exponent 2 emerges [18]. In Ref. [15], we investigated our hypothesis using coupled dynamical system models and discovered that strong coupling induces a type of synchronization where time series become mutually proportional, resulting in TL with an exponent 2. We refer to this type of synchronization as *waveform proportionality* (WP). Although synchronization characterized by proportional time series has been previously reported as projective synchronization [19] or as a specific instance of generalized synchronization [20], these observations were confined to particular classes of models. More recently, we demonstrated that this type of synchronization can manifest in a broader range of models [15]. In Ref. [15], we employed the coupled food chain model [21–23], the coupled Rössler system [23–28], the coupled Brusselator [29], and the coupled Lorenz system [30]. For the initial three models, we elucidated the mechanism of TL using a perturbative method and an averaging approximation. In contrast, the coupled Lorenz system necessitated a self-consistent approach instead of the averaging method. In this paper, we extend our previous results for the coupled Lorenz system and provide detailed calculations. We present results not only for the coupled Lorenz system [30] which is based on the original Lorenz system [31], but also for coupled systems constructed from the generalized Lorenz system [32, 33] and the hyperchaotic Lorenz system [34]. The generalized Lorenz system, an extension of the original Lorenz system incorporating the influence of a magnetic field [32], has been shown to exhibit intriguing intermittent dynamics [33]. The hyperchaotic Lorenz system [34], also an extension of the original Lorenz system, displays more complex dynamics

* mitsui@design.kyushu-u.ac.jp

than the original Lorenz system [31] and is of particular interest for applications in secure communication and cryptography.

II. ORIGINAL LORENZ SYSTEM

A. Model

First, we present the results for the original Lorenz system [31]:

$$\dot{x} = \sigma(y - x), \quad (2a)$$

$$\dot{y} = x(\rho - z) - y, \quad (2b)$$

$$\dot{z} = xy - bz. \quad (2c)$$

Using this system, we construct the following coupled system [30]:

$$\dot{x}_i = \sigma(y_i - x_i) + aw_i + D_x(X - x_i), \quad (3a)$$

$$\dot{y}_i = x_i(\rho_i - z_i) - y_i + D_y(Y - y_i), \quad (3b)$$

$$\dot{z}_i = x_i y_i - bz_i + D_z(Z - z_i), \quad (3c)$$

where D_x , D_y , and D_z are coupling coefficients, and $X = \langle x_i \rangle_i$, $Y = \langle y_i \rangle_i$, and $Z = \langle z_i \rangle_i$. The notation $\langle \cdot \rangle_i$ denotes the ensemble average, namely, $\langle v_i \rangle_i = (1/N) \sum_{i=1}^N v_i$ ($v_i = x_i, y_i, z_i$). The parameter ρ_i is defined as

$$\rho_i = \rho_0 + \mu_i, \quad (4a)$$

$$\langle \mu_i \rangle_i = 0. \quad (4b)$$

Eq. (4) is satisfied by setting $\rho_0 = \langle \rho_i \rangle_i$.

In Sec. II–B, we analytically demonstrate that, under strong coupling, WP and TL (defined below) arise in the variable $z_i(t)$. We consider a time-series set $z_i(t)$ ($i = 1, \dots, N$). For temporal TL, we compute the mean and variance for each oscillator i as $E[z_i(t)]_t = \langle z_i(t) \rangle_t$ and $V[z_i(t)]_t = \langle (z_i(t) - E[z_i(t)]_t)^2 \rangle_t$, respectively, where $\langle \cdot \rangle_t$ denotes the long-time average or the average over one cycle when $z_i(t)$ is periodic. A linear fitting to N data points of $(\log E[z_i(t)]_t, \log V[z_i(t)]_t)$ yields the slope β_t and intercept $\log \alpha_t$. For spatial TL, the mean and variance at time t are given by $E[z_i(t)]_i = \langle z_i(t) \rangle_i$ and $V[z_i(t)]_i = \langle (z_i(t) - E[z_i(t)]_i)^2 \rangle_i$, respectively, where $\langle \cdot \rangle_i$ denotes the average over oscillator i . A linear fitting to M data points $(\log E[z_i(t)]_i, \log V[z_i(t)]_i)$, where M is the number of sample times, yields the slope β_s and intercept $\log \alpha_s$. In both cases, R^2 denotes the coefficient of determination for the linear fitting. When WP holds, TL with an exponent 2 naturally arises, as shown below. WP is defined by the following relation:

$$z_i(t) = C_i z_0(t). \quad (5)$$

Under this condition, the temporal mean, temporal variance, ensemble mean, and ensemble variance of $z_i(t)$ are given by

$$E[z_i(t)]_t = C_i E[z_0(t)]_t, \quad (6)$$

$$V[z_i(t)]_t = C_i^2 V[z_0(t)]_t, \quad (7)$$

$$E[z_i(t)]_i = E[C_i]_i z_0(t), \quad (8)$$

$$V[z_i(t)]_i = V[C_i]_i [z_0(t)]^2. \quad (9)$$

By eliminating C_i from Eqs. (6) and (7), and $z_0(t)$ from Eqs. (8) and (9), we obtain the following relationships:

$$V[z_i(t)]_t = \frac{V[z_0(t)]_t}{E[z_0(t)]_t^2} E[z_i(t)]_t^2, \quad (10)$$

$$V[z_i(t)]_i = \frac{V[C_i]_i}{E[C_i]_i^2} E[z_i(t)]_i^2. \quad (11)$$

These equations represent temporal and spatial TLs with an exponent 2, respectively. In practice, WP as given by Eq. (5) may include a time delay and is more accurately described by:

$$z_i(t) = C_i z_0(t - t_i), \quad (12)$$

where t_i is a time delay that depends on the coupling strength and decreases as the coupling becomes stronger. Under the condition described by Eq. (12), the relation (10) still holds, whereas the relation (11) does not. Therefore, the emergence of spatial TL requires stronger coupling than that needed for temporal TL [15].

B. Analytical derivation

To demonstrate that WP and TL with an exponent 2 hold for $z_i(t)$, we approximately solve the coupled Lorenz system described by Eq. (3). Following Ref. [15], we consider the expansion:

$$x_i(t) = x_0(t - \varepsilon_i \tau) + \varepsilon_i p(t - \varepsilon_i \tau) + O(\varepsilon_i^2), \quad (13a)$$

$$y_i(t) = y_0(t - \varepsilon_i \tau) + \varepsilon_i q(t - \varepsilon_i \tau) + O(\varepsilon_i^2), \quad (13b)$$

$$z_i(t) = z_0(t - \varepsilon_i \tau) + \varepsilon_i r(t - \varepsilon_i \tau) + O(\varepsilon_i^2), \quad (13c)$$

where $\varepsilon_i = \mu_i/D_x$ is a nondimensional small parameter; τ is a constant; $p(t)$, $q(t)$, and $r(t)$ are functions to be determined; $\hat{\varepsilon}$ represents the typical magnitude of the small parameter ε_i ; and x_0 , y_0 , and z_0 constitute a reference oscillator satisfying

$$\dot{x}_0 = \sigma(y_0 - x_0), \quad (14a)$$

$$\dot{y}_0 = x_0(\rho_0 - z_0) - y_0, \quad (14b)$$

$$\dot{z}_0 = x_0 y_0 - bz_0. \quad (14c)$$

Our objective is to show that $r(t) \propto z_0(t)$ holds in a good approximation for sufficiently small $\hat{\varepsilon}$ and sufficiently large D_x . If $r(t) \propto z_0(t)$ is approximately true, then WP, i.e., $z_1(t) \propto \dots \propto z_N(t)$, also holds approximately. When $|\sigma(y_0 - x_0)| \gg |\mu_i p|, |\varepsilon_i \sigma q|, |\mu_i \tau \sigma(y_0 - x_0)|$, substituting Eq. (13) into Eq. (3) and extracting $O(\varepsilon_i)$ terms from both sides, we obtain

$$\dot{p} = -(\sigma + D_x)p + \sigma q + D_x \tau \sigma(y_0 - x_0), \quad (15a)$$

$$\begin{aligned} \dot{q} = & -(1 + D_y)q + (D_x - r)x_0 + (\rho_0 - z_0)p \\ & + D_y\tau x_0(\rho_0 - z_0) - D_y\tau y_0, \end{aligned} \quad (15b)$$

$$\dot{r} = -(b + D_z)r + py_0 + qx_0 + D_z\tau x_0 y_0 - D_z\tau b z_0. \quad (15c)$$

When D_x is sufficiently large, p is a fast variable, and we may adiabatically eliminate p from the system in a good approximation. Solving $\dot{p} = 0$, we find

$$p = \frac{\sigma q + D_x\tau\sigma(y_0 - x_0)}{\sigma + D_x}. \quad (16)$$

Substituting Eq. (16) into Eqs. (15b) and (15c), assuming that q and r are $O(D_x)$, and then eliminating terms smaller than $O(D_x)$, Eqs. (15b) and (15c) can be approximated to

$$\dot{q} = -(1 + D_y)q + (D_x - r)x_0, \quad (17a)$$

$$\dot{r} = -(b + D_z)r + qx_0. \quad (17b)$$

Assuming that $r(t)$ is $O(D_x)$, Eq. (17a) implies that $q(t)$ is also $O(D_x)$. Then, Eq. (17b) confirms that $r(t)$ is indeed $O(D_x)$. We now consider the case where there are no couplings in the variables y_i and z_i (i.e., $D_y = D_z = 0$), or when the couplings are weak ($D_y \ll 1$ and $D_z \ll b$). In these cases, the equations simplify to

$$\dot{q} = -q + (D_x - r)x_0, \quad (18a)$$

$$\dot{r} = -br + qx_0. \quad (18b)$$

From Eqs. (14b), (14c), (18a), and (18b), the following proportional relationships are obtained:

$$q(t) = \frac{D_x}{\rho_0} y_0(t), \quad (19)$$

$$r(t) = \frac{D_x}{\rho_0} z_0(t). \quad (20)$$

Thus, $r(t) \propto z_0(t)$, which implies that WP holds for $z_i(t)$. Consequently, the theoretical predictions for the intercepts and exponents of temporal and spatial TLs are given by

$$\log \alpha_t = \log \frac{\text{Var}[z_0(t)]_t}{\text{E}[z_0(t)]_t^2}, \quad (21a)$$

$$\beta_t = 2, \quad (21b)$$

$$\log \alpha_s = \log \frac{\text{Var}[\mu_i]_i}{\rho_0^2}, \quad (21c)$$

$$\beta_s = 2. \quad (21d)$$

C. Numerical simulations

In this section, we validate the analytical derivation through numerical simulations. Before proceeding, we introduce two quantities, χ and $\zeta_i(t)$, to quantify the degree of synchronization between time series and to assess the presence of WP, respectively:

$$\chi = \frac{\text{CV}[Z(t)]}{\max_i \{\text{CV}[z_i(t)]\}}, \quad (22)$$

$$\zeta_i(t) = \frac{z_i(t)}{z_j(t)}, \quad (23)$$

where CV denotes the coefficient of variation. Namely, χ is the CV of the mean field of $z_i(t)$ normalized by the maximum CV among the individual $z_i(t)$. With this definition, $0 \leq \chi \leq 1$, where $\chi \simeq 0$ indicates an unsynchronized state and $\chi \simeq 1$ signifies a well-synchronized state. The quantity $\zeta_i(t)$ represents the ratio between time series; it becomes approximately constant when WP holds. While the choice of j is arbitrary, we select $j = 50$, assuming the parameters μ_i satisfy $\mu_1 < \mu_2 < \dots < \mu_{100}$. By arranging them in this manner, we can expect $z_{50}(t) \simeq z_0(t)$. Unless otherwise noted, μ_i is selected from a uniform distribution between -1.5 and 1.5 .

First, using the coupled Lorenz system [30], we confirm that WP and TL with an exponent 2 are observed for sufficiently large D_x . Figure 1 shows that without coupling, the time series are not synchronized, WP does not hold, and temporal and spatial TLs with an exponent 2 are not observed. In contrast, with sufficiently strong coupling, the time series become well synchronized, WP holds, and temporal and spatial TLs with an exponent 2 are clearly observed.

Next, we examine the dependence of the TL parameters on the coupling strength. According to the analytical derivation, the numerical simulation results are expected to agree well with the theoretical predictions as D_x increases. We verify this expectation using the coupled Lorenz system [30]; the results are shown in Fig. 2. Simulations are performed up to $t = 3500$, and TL is computed using the time series from $t = 3000$ to $t = 3500$. The error bars represent the standard deviation of ten calculations with different initial conditions and realizations of ρ_i . Initial conditions for numerical simulations are randomly chosen from a uniform distribution between 0 and 1. Depending on the coupling strength, oscillation quenching may occur, rendering it impossible to define χ . Thus, we judge that oscillation quenching occurs when $(1/N) \sum_{i=1}^N \langle (z_i - \langle z_i \rangle_t)^2 \rangle_t$ falls below a certain threshold value; such cases are excluded. We can confirm that qualitatively the same results are obtained for several different threshold values. This procedure is applied to all systems described later. Figure 2 illustrates that when the coupling strength D_x becomes comparable to $\max\{\mu_i\}$, χ begins to rise, indicating the onset of synchronization. With a further increase in coupling strength, $\chi \simeq 1$ and $R^2 \simeq 1$, and the theoretical predictions and numerical simulation results for both $\log \alpha_{t,s}$ and $\beta_{t,s}$ show excellent agreement.

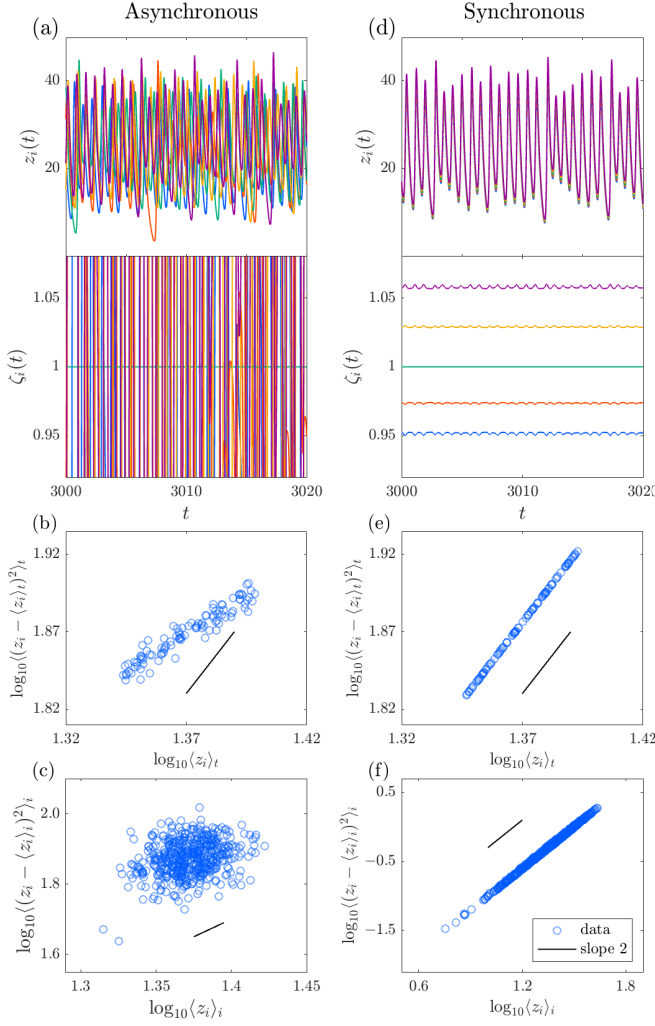


FIG. 1. Examples of WP and TL in the coupled Lorenz system. $N = 100$, $D_y = D_z = 0$, $\sigma = 10$, $b = 8/3$, and ρ_i is randomly selected from a uniform distribution between 26.5 and 29.5. In panels (a) and (d), data for $i = 1, 25, 50, 75$, and 100 are shown. (a) $z_i(t)$ (upper) and $\zeta_i(t)$ (bottom) for $D_x = 0$. (b) Temporal TL for $D_x = 0$. (c) Spatial TL for $D_x = 0$. (d) $z_i(t)$ (upper) and $\zeta_i(t)$ (bottom) for $D_x = 1000$. (e) Temporal TL for $D_x = 1000$. (f) Spatial TL for $D_x = 1000$.

III. GENERALIZED AND HYPERCHAOTIC LORENZ SYSTEMS

A. Model

Our analysis can be extended to the generalized Lorenz system [32, 33] and the hyperchaotic Lorenz system [34]. The generalized Lorenz system is described as follows.

$$\dot{x} = \sigma(y - x) - \omega_0 w, \quad (24a)$$

$$\dot{y} = x(\rho - z) - y, \quad (24b)$$

$$\dot{z} = xy - bz, \quad (24c)$$

$$\dot{w} = \omega_0 x - \sigma_m w, \quad (24d)$$

where $w(t)$, ω_0 , and σ_m represent a variable and parameters associated with the magnetic field. The hyperchaotic Lorenz system is described as follows.

$$\dot{x} = \sigma(y - x) + w, \quad (25a)$$

$$\dot{y} = x(\rho - z) - y, \quad (25b)$$

$$\dot{z} = xy - bz, \quad (25c)$$

$$\dot{w} = -yz + \gamma w, \quad (25d)$$

where $w(t)$ is a nonlinear controller and γ is a newly introduced parameter. To treat these systems within a unified formulation, we introduce the following system:

$$\dot{x} = \sigma(y - x) + aw, \quad (26a)$$

$$\dot{y} = x(\rho - z) - y, \quad (26b)$$

$$\dot{z} = xy - bz, \quad (26c)$$

$$\dot{w} = cx - ky - lw, \quad (26d)$$

where $x(t)$, $y(t)$, and $z(t)$ are the original variables of the Lorenz system, and σ , ρ , and b are its original parameters. The variable $w(t)$ and parameters a , c , k , and l are newly introduced to extend the original Lorenz system. By appropriately choosing the parameters a , c , k , and l , we can recover the original/generalized/hyperchaotic Lorenz system; when $a = c = k = l = 0$, the system reduces to the original Lorenz system (2); when $a = -\omega_0$, $c = \omega_0$, $k = 0$, and $l = \sigma_m$, it corresponds to the generalized Lorenz system (24); and when $a = 1$, $c = 0$, $k = 1$, and $l = -\gamma$, it corresponds to the hyperchaotic Lorenz system (25). We refer to the system described by Eq. (26) as the extended Lorenz system. Following the formulation of the coupled Lorenz system used in Ref. [30], we construct the following coupled system for the extended Lorenz system:

$$\dot{x}_i = \sigma(y_i - x_i) + aw_i + D_x(X - x_i), \quad (27a)$$

$$\dot{y}_i = x_i(\rho_i - z_i) - y_i + D_y(Y - y_i), \quad (27b)$$

$$\dot{z}_i = x_i y_i - bz_i + D_z(Z - z_i), \quad (27c)$$

$$\dot{w}_i = cx - ky - lw + D_w(W - w_i), \quad (27d)$$

where D_w is a coupling coefficient, and $W = \langle w_i \rangle_i$. The parameter ρ_i is defined as Eq. (4).

B. Analytical derivation

To show that WP and TL with an exponent 2 also hold for $z_i(t)$ in the generalized and hyperchaotic Lorenz systems, we approximately solve the coupled extended Lorenz system described by Eq. (27). Following Ref. [15], we consider the expansion:

$$x_i(t) = x_0(t - \varepsilon_i \tau) + \varepsilon_i p(t - \varepsilon_i \tau) + O(\varepsilon^2), \quad (28a)$$

$$y_i(t) = y_0(t - \varepsilon_i \tau) + \varepsilon_i q(t - \varepsilon_i \tau) + O(\varepsilon^2), \quad (28b)$$

$$z_i(t) = z_0(t - \varepsilon_i \tau) + \varepsilon_i r(t - \varepsilon_i \tau) + O(\varepsilon^2), \quad (28c)$$

$$w_i(t) = w_0(t - \varepsilon_i \tau) + \varepsilon_i s(t - \varepsilon_i \tau) + O(\varepsilon^2), \quad (28d)$$

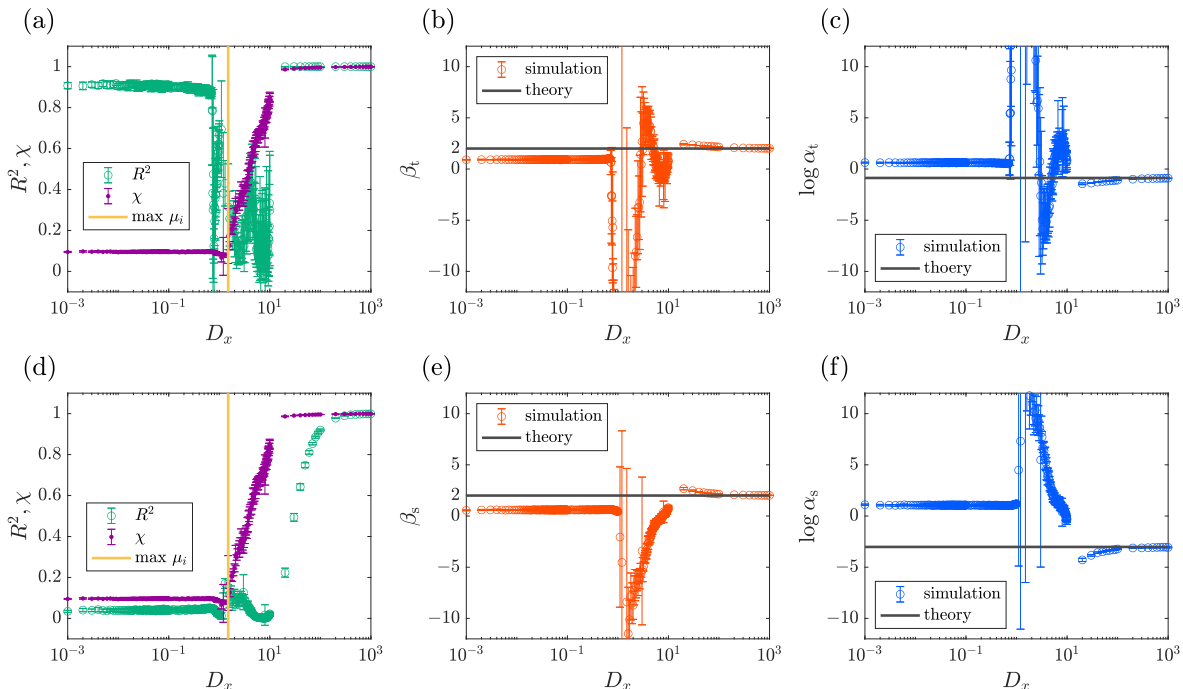


FIG. 2. Dependence of TL parameters and synchronization degree on D_x in the coupled Lorenz system. $D_y = D_z = 0$, $N = 100$, $\sigma = 10$, $b = 8/3$, and ρ_i is randomly selected from a uniform distribution between 26.5 and 29.5. In panels (a) and (d), the same χ (purple dot) and $\max\{\mu_i\}$ (orange solid line) are plotted. (a) R^2 of temporal TL. (b) Exponents of temporal TL. (c) Intercepts of temporal TL. (d) R^2 of spatial TL. (e) Exponents of spatial TL. (f) Intercepts of spatial TL.

where x_0 , y_0 , z_0 , and w_0 constitute a reference oscillator satisfying

$$\dot{x}_0 = \sigma(y_0 - x_0) + aw_0, \quad (29a)$$

$$\dot{y}_0 = x_0(\rho_0 - z_0) - y_0, \quad (29b)$$

$$\dot{z}_0 = x_0y_0 - bz_0, \quad (29c)$$

$$\dot{w}_0 = cx_0 - ky_0z_0 - lw_0. \quad (29d)$$

When $|\sigma(y_0 - x_0)|, |aw_0| \gg |\mu_i p|, |\varepsilon_i \sigma q|, |\mu_i \tau \sigma(y_0 - x_0)|, |\mu_i \tau aw_0|$, the following equations can be derived by applying the same procedure as before.

$$\dot{q} = -q + (D_x - r)x_0, \quad (30a)$$

$$\dot{r} = -br + qx_0, \quad (30b)$$

$$\dot{s} = -(l + D_w)s - kry_0 - kz_0. \quad (30c)$$

Again, from Eqs. (29b), (29c), (30a), and (30b), the proportional relationships as shown in Eqs. (19) and (20) are obtained. For the coupled extended Lorenz system, the theoretical predictions for the intercept and exponent values of TL are also given by Eq. (21).

C. Numerical simulations

As shown in Figs. 3 and 4, results similar to those obtained for the coupled Lorenz system are also observed in

the coupled generalized Lorenz system and the coupled hyperchaotic Lorenz system. In both cases, the exponent of TL approaches 2 in the large D_x regime, and the intercept also shows good agreement with the theoretical prediction.

Thus far, we have confirmed good agreement between analytical predictions and numerical simulations for several models. In all cases, the system parameters were chosen such that the systems exhibited chaotic behavior. The results of the analytical calculations, however, do not depend on whether the system dynamics are chaotic or periodic. Therefore, we next verify, using the coupled generalized Lorenz system, that WP and TL with an exponent 2 also emerge when the system exhibits periodic behavior, in addition to chaotic dynamics. Since the generalized Lorenz system is known to exhibit intermittent chaos for certain parameter values [33], we also include results obtained under parameter settings that lead to intermittent chaos. As shown in Fig. 5, WP and TL with an exponent 2 are clearly observed when D_x is sufficiently large, regardless of whether the dynamics are periodic, chaotic, or intermittent. Next, we investigate the effects of the other coupling coefficients, D_y , D_z , and D_w , on the validity of the theory. Based on the analytical derivation, we expect that the theoretical framework to become invalid when D_y or D_z is non-negligible. In contrast, our theory predicts that increasing D_w does not affect the results. To test these expectations, we

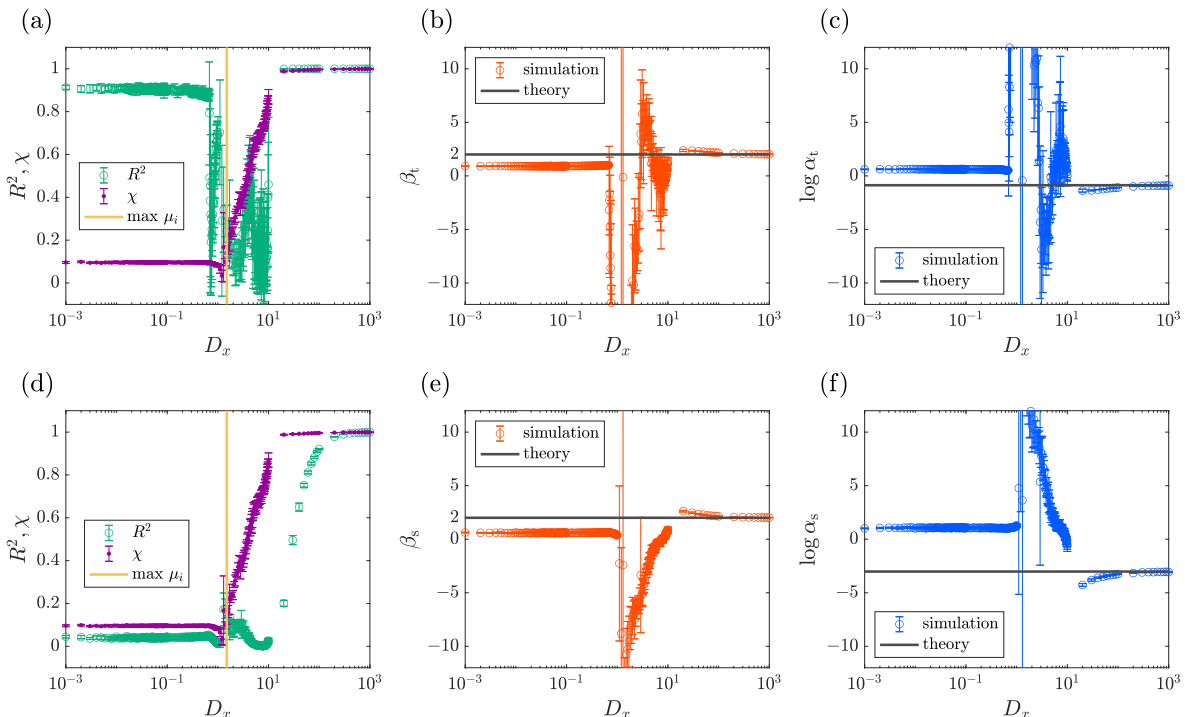


FIG. 3. Dependence of TL parameters and synchronization degree on D_x in the coupled generalized Lorenz system. $a = -1, c = 1, k = 0, l = 20$ and $D_y = D_z = D_w = 0$. $N = 100, \sigma = 10, b = 8/3$, and ρ_i is randomly selected from a uniform distribution between 26.5 and 29.5. In panels (a) and (d), the same χ (purple dot) and $\max\{\mu_i\}$ (orange solid line) are plotted. (a) R^2 of temporal TL. (b) Exponents of temporal TL. (c) Intercepts of temporal TL. (d) R^2 of spatial TL. (e) Exponents of spatial TL. (f) Intercepts of spatial TL.

perform numerical simulations using the coupled hyperchaotic Lorenz system (Figs. 6, 7, and 8). As shown in Fig. 6, when D_y becomes non-negligible compared to 1, although R^2 for temporal TL remains close to 1, β_t and $\log \alpha_t$ begin to deviate from the theoretical predictions, indicating a breakdown of WP. For spatial TL, when D_y is non-negligible relative to 1, R^2 falls below 1, and both β_s and $\log \alpha_s$ also deviate from the theoretical predictions, further confirming that WP no longer holds. We can confirm that qualitatively the same behavior is observed when D_z becomes non-negligible compared to b (Fig. 7). Furthermore, as expected, we confirm that increasing D_w does not affect the emergence of TL with an exponent 2 (Fig. 8).

IV. DISCUSSION

In this study, building upon our previous work [15], we investigated the emergence of WP and the associated TL with an exponent 2 in coupled Lorenz systems. In particular, we extended the results obtained in Ref. [15] by considering a coupled system constructed from the extended Lorenz system (26), which is newly introduced in this study. We verified our analytical derivation through

numerical simulations using coupled systems constructed from the original, generalized, and hyperchaotic Lorenz systems. In the case of the four-variable model, we numerically observe that $|aw_0|$ is not always large and our assumption of large $|aw_0|$ in our perturbative approach might be violated. Nevertheless, the numerical simulation results are still in good agreement with the theoretical predictions. This observation suggests that the treatment of the aw_0 term in our perturbative approach requires further consideration.

By combining this study with Ref. [15], we provide broader evidence supporting the generality of WP and TL with an exponent 2 in strongly coupled systems. Although several mechanisms have been proposed in the literature to explain the emergence of TL with an exponent 2 [11, 12, 14, 35–41], the present paper and Ref. [15] suggest that synchronization, a universal phenomenon [42], underlies TL, another universal phenomenon.

The phenomenon in which time series are proportional to each other has previously been reported using a coupled Lorenz system [19]. However, in this study, we have shown that this type of synchronization also appears not only in the original Lorenz system but also in the generalized and hyperchaotic Lorenz systems, thereby extending the scope of this phenomenon.

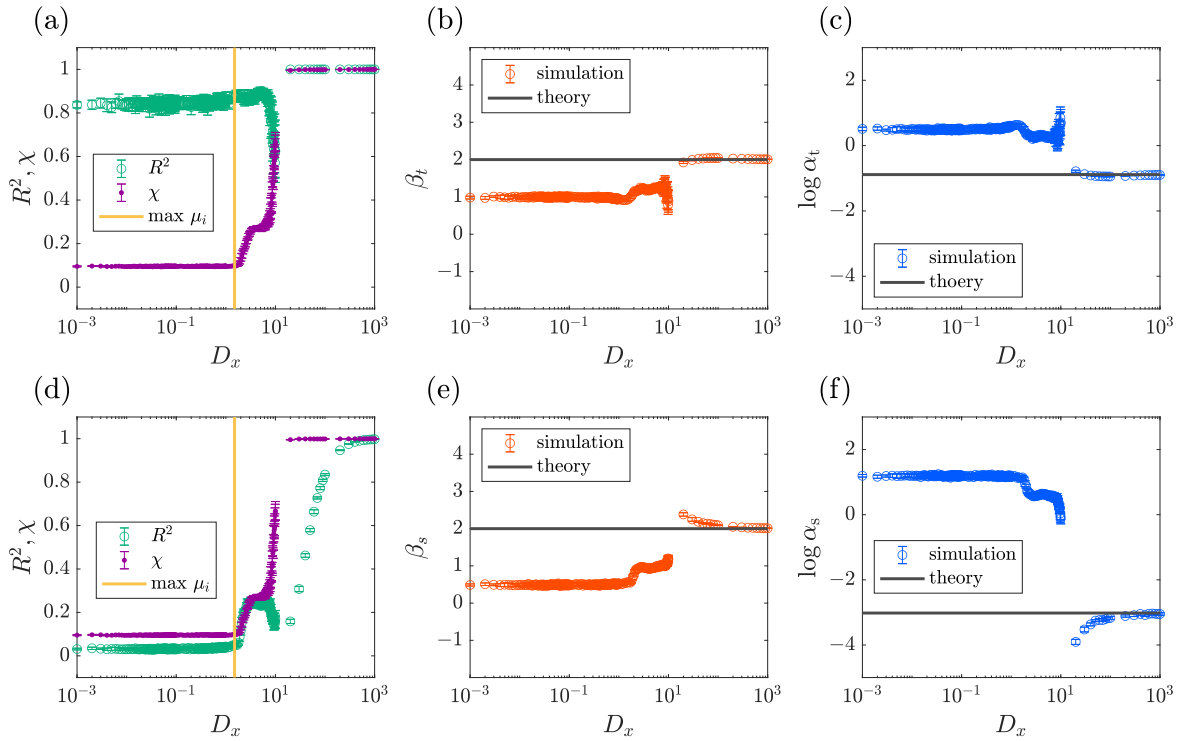


FIG. 4. Dependence of TL parameters and synchronization degree on D_x in the coupled hyperchaotic Lorenz system. $a = 1, c = 0, k = 1, l = 1$ and $D_y = D_z = D_w = 0$. $N = 100, \sigma = 10, b = 8/3$, and ρ_i is randomly selected from a uniform distribution between 26.5 and 29.5. In panels (a) and (d), the same χ (purple dot) and $\max\{\mu_i\}$ (orange solid line) are plotted. (a) R^2 of temporal TL. (b) Exponents of temporal TL. (c) Intercepts of temporal TL. (d) R^2 of spatial TL. (e) Exponents of spatial TL. (f) Intercepts of spatial TL.

-
- [1] C. I. Bliss, Statistical problems in estimating populations of Japanese beetle larvae, *J. Econ. Entomol.* **34** (34).
- [2] L. R. Taylor, Aggregation, variance and the mean, *Nature* **189**, 732–735 (1961).
- [3] Z. Eisler, I. Bartos, and J. Kertész, Fluctuation scaling in complex systems: Taylor’s law and beyond, *Advances in Physics* **57**, 89–142 (2008).
- [4] R. A. J. Taylor, *Taylor’s Power Law: Order and Pattern in Nature*, 1st ed. (Academic Press, 2019).
- [5] F. Ginelli, The physics of the Vicsek model, *Eur. Phys. J. Special Topics* **225**, 2099–2117 (2016).
- [6] H. Chaté, Dry aligning dilute active matter, *Annu. Rev. Condens. Matter Phys.* **11**, 189–212 (2019).
- [7] D. Nishiguchi, Deciphering long-range order in active matter: Insights from swimming bacteria in quasi-2D and electrokinetic Janus particles, *J. Phys. Soc. Jpn.* **92**, 121007 (2023).
- [8] L. R. Taylor and I. P. Woiwod, Comparative synoptic dynamics. I. Relationships between inter- and intra-specific spatial and temporal variance/mean population parameters, *Source: J. Anim. Ecol.* **51**, 879–906 (1982).
- [9] A. J. Kerkhoff and F. B. IV, The scaling of reproductive variability in trees, *Ecol. Lett.* **6**, 850–856 (2003).
- [10] L. Zhao, L. W. Sheppard, P. C. Reid, J. A. Walter, and D. C. Reuman, Proximate determinants of Taylor’s law slopes, *J. Anim. Ecol.* **88**, 484–494 (2019).
- [11] J. E. Cohen, M. Xu, and W. S. Schuster, Stochastic multiplicative population growth predicts and interprets Taylor’s power law of fluctuation scaling, *Proc. R. Soc. B* **280** (2013).
- [12] J. E. Cohen, Taylor’s law and abrupt biotic change in a smoothly changing environment, *Theor. Ecol.* **7**, 77–86 (2014).
- [13] J. E. Cohen, Stochastic population dynamics in a Markovian environment implies Taylor’s power law of fluctuation scaling, *Theor. Popul. Biol.* **93**, 30–37 (2014).
- [14] A. Giometto, M. Formentin, A. Rinaldo, J. E. Cohen, and A. Maritan, Sample and population exponents of generalized Taylor’s law, *Proc. Natl. Acad. Sci. U.S.A.* **112**, 7755–7760 (2015).
- [15] Y. Mitsui and H. Kori, Waveform proportionality and Taylor’s law induced by synchronization of periodic and chaotic oscillators, *Phys. Rev. Lett.* **134**, 167202 (2025).
- [16] F. B. IV and A. J. Kerkhoff, Reproductive correlation and mean-variance scaling of reproductive output for a forest model, *J. Theor. Biol.* **235**, 373–380 (2005).
- [17] I. Hanski, Cross-correlation in population dynamics and the slope of spatial variance: Mean regressions, *Oikos* **50**, 148–151 (1987).
- [18] D. C. Reuman, L. Zhao, L. W. Sheppard, P. C. Reid,

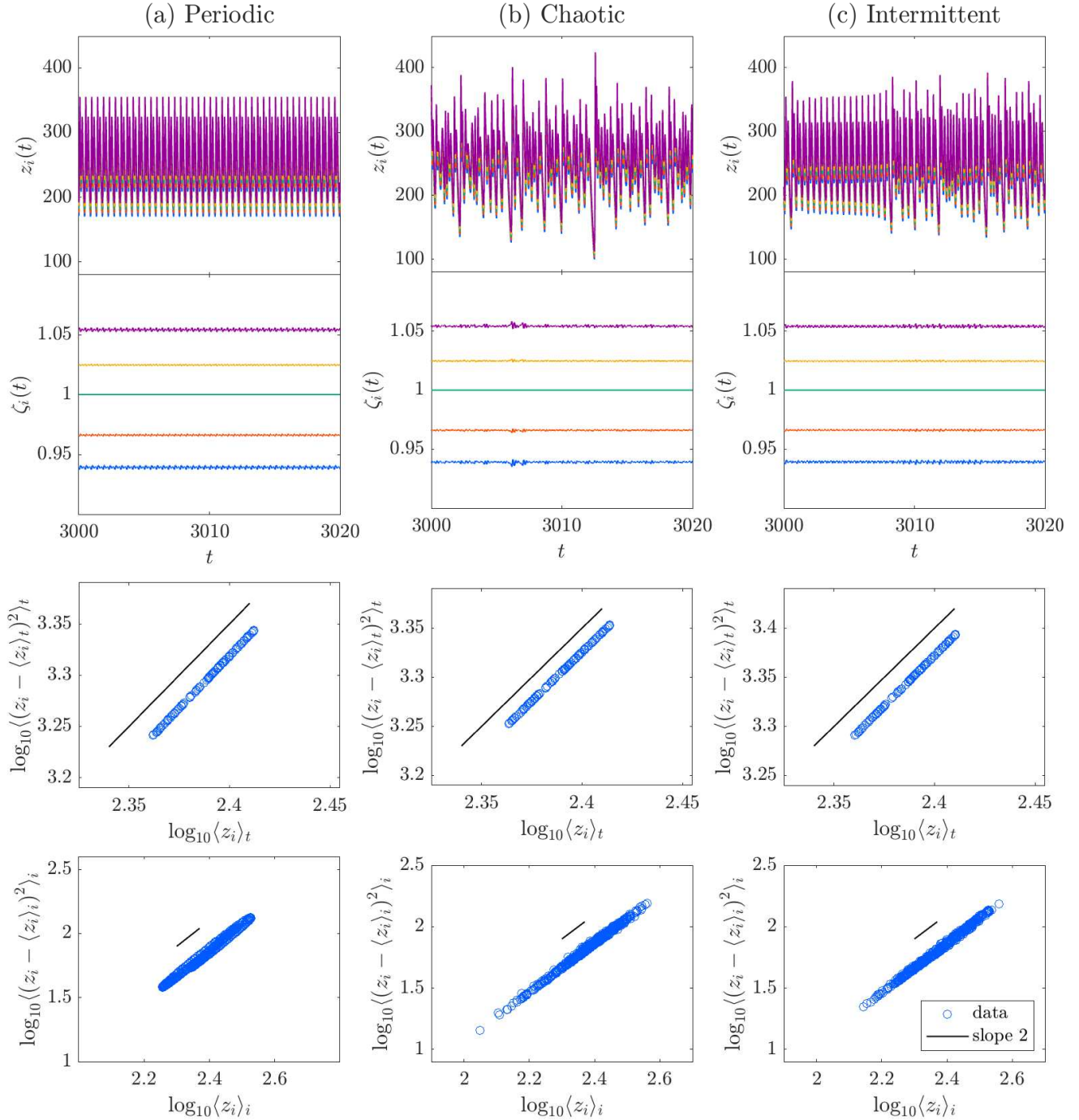


FIG. 5. Examples of WP and TL in the coupled generalized Lorenz system. $a = -\omega_0$, $c = \omega_0$, $k = 0$, $l = 1$, $D_x = 1000$, and $D_y = D_z = D_w = 0$. $N = 100$, $\sigma = 10$, $b = 8/3$, and ρ_i is randomly selected from a uniform distribution between 241 and 271 (namely, μ_i is selected from a uniform distribution between -15 and 15). For $z_i(t)$ and $\zeta_i(t)$, data for $i = 1, 25, 50, 75$, and 100 are shown. (a) Periodic: $\omega_0 = 1$. (b) Chaotic: $\omega_0 = 10$. (c) Intermittent: $\omega_0 = 3.74$.

and J. E. Cohen, Synchrony affects Taylor's law in theory and data, Proc. Natl. Acad. Sci. U.S.A. **114**, 6788–6793 (2017).

[19] R. Mainieri and J. Rehacek, Projective synchronization in three-dimensional chaotic systems, Phys. Rev. Lett. **82** (1999).

[20] T. Kano and K. Umeno, Chaotic synchronization of mutually coupled systems-arbitrary proportional linear relations, Chaos **32** (2022).

[21] B. Blasius, A. Huppert, and L. Stone, Complex dynamics and phase synchronization in spatially extended ecological systems, Nature **399**, 354–359 (1999).

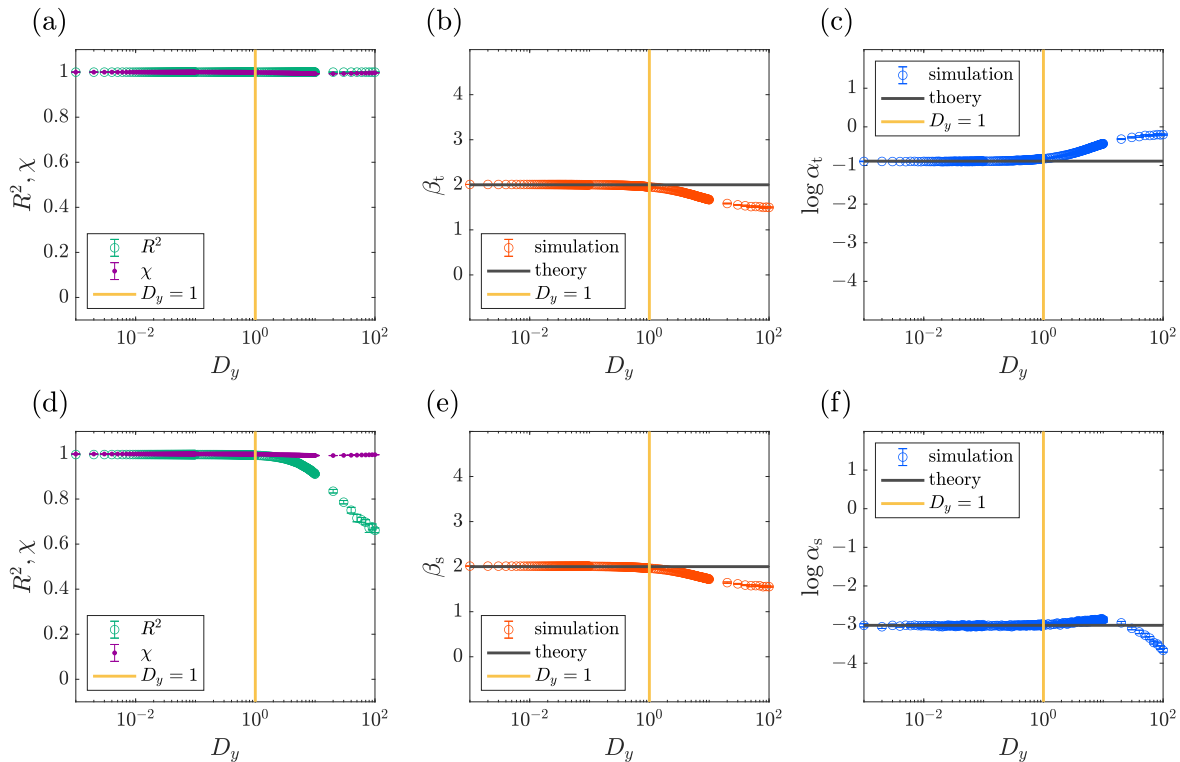


FIG. 6. Dependence of TL parameters on D_y in the coupled hyperchaotic Lorenz system. $a = 1, c = 0, k = 1, l = 1$ and $D_x = 1000, D_z = D_w = 0$. $N = 100, \sigma = 10, b = 8/3$, and ρ_i is randomly selected from a uniform distribution between 26.5 and 29.5. (a) R^2 of temporal TL. (b) Exponents of temporal TL. (c) Intercepts of temporal TL. (d) R^2 of spatial TL. (e) Exponents of spatial TL. (f) Intercepts of spatial TL.

- [22] B. Blasius and L. Stone, Chaos and phase synchronization in ecological systems, *Int. J. Bifurcation Chaos* **10** (2000).
- [23] E. Montbrió and B. Blasius, Using nonisochronicity to control synchronization in ensembles of nonidentical oscillators, *Chaos* **13**, 291–308 (2003).
- [24] M. G. Rosenblum, A. S. Pikovsky, and J. Kurths, Phase synchronization of chaotic oscillators, *Phys. Rev. Lett.* (1996).
- [25] M. G. Rosenblum, A. S. Pikovsky, and J. Kurths, From phase to lag synchronization in coupled chaotic oscillators, *Phys. Rev. Lett.* **78**, 4193–4196 (1997).
- [26] H. Sakaguchi, Phase transition in globally coupled Rössler oscillators, *Phys. Rev. E* **61**, 7212–7214 (2000).
- [27] A. S. Pikovsky, M. G. Rosenblum, and J. Kurth, Synchronization in a population of globally coupled chaotic oscillators, *Europhys. Lett.* **34**, 165–170 (1996).
- [28] G. V. Osipov, A. S. Pikovsky, M. G. Rosenblum, and J. R. Kurths, Phase synchronization effects in a lattice of nonidentical Rössler oscillators, *Phys. Rev. E* **55**, 2353–2361 (1997).
- [29] H. Daido, Strong-coupling limit in heterogeneous populations of coupled oscillators, *Phys. Rev. E* **84** (2011).
- [30] K. J. Lee, Y. Kwak, and T. K. Lim, Phase jumps near a phase synchronization transition in systems of two coupled chaotic oscillators, *Phys. Rev. Lett.* **81**, 321–324 (1998).
- [31] E. N. Lorenz, Deterministic nonperiodic flow, *J. Atmos. Sci.* **20**, 130–141 (1963).
- [32] W. M. Macek and M. Strumik, Model for hydromagnetic convection in a magnetized fluid, *Phys. Rev. E* **82** (2010).
- [33] W. M. Macek and M. Strumik, Hyperchaotic intermittent convection in a magnetized viscous fluid, *Phys. Rev. Lett.* **112** (2014).
- [34] X. Wang and M. Wang, A hyperchaos generated from Lorenz system, *Physica A* **387**, 3751–3758 (2008).
- [35] J. E. Cohen, Taylor’s power law of fluctuation scaling and the growth-rate theorem, *Theor. Popul. Biol.* **88**, 94–100 (2013).
- [36] A. S. Sassi, M. Garcia-Alcala, M. Aldana, and Y. Tu, Protein concentration fluctuations in the high expression regime: Taylor’s law and its mechanistic origin, *Phys. Rev. X* **12**, 011051 (2022).
- [37] A. M. Kilpatrick and A. R. Ives, Species interactions can explain Taylor’s power law for ecological time series, *Nature* **422**, 65–68 (2003).
- [38] R. M. Anderson, D. M. Gordon, M. J. Crawley, and M. P. Hassel, Variability in the abundance of animal and plant species, *Nature* **296**, 245–248 (1982).
- [39] M. Salahshour, Predator-prey power laws: trophic interactions give rise to scale-invariant ecosystems, *New J. Phys.* (2023).
- [40] F. B. IV, The upper limit for the exponent of Taylor’s power law is a consequence of deterministic population growth, *Evol. Ecol. Res.* **7**, 1213–1220 (2005).
- [41] S. Carpenter, S. Callens, C. Brown, J. E. Cohen, and

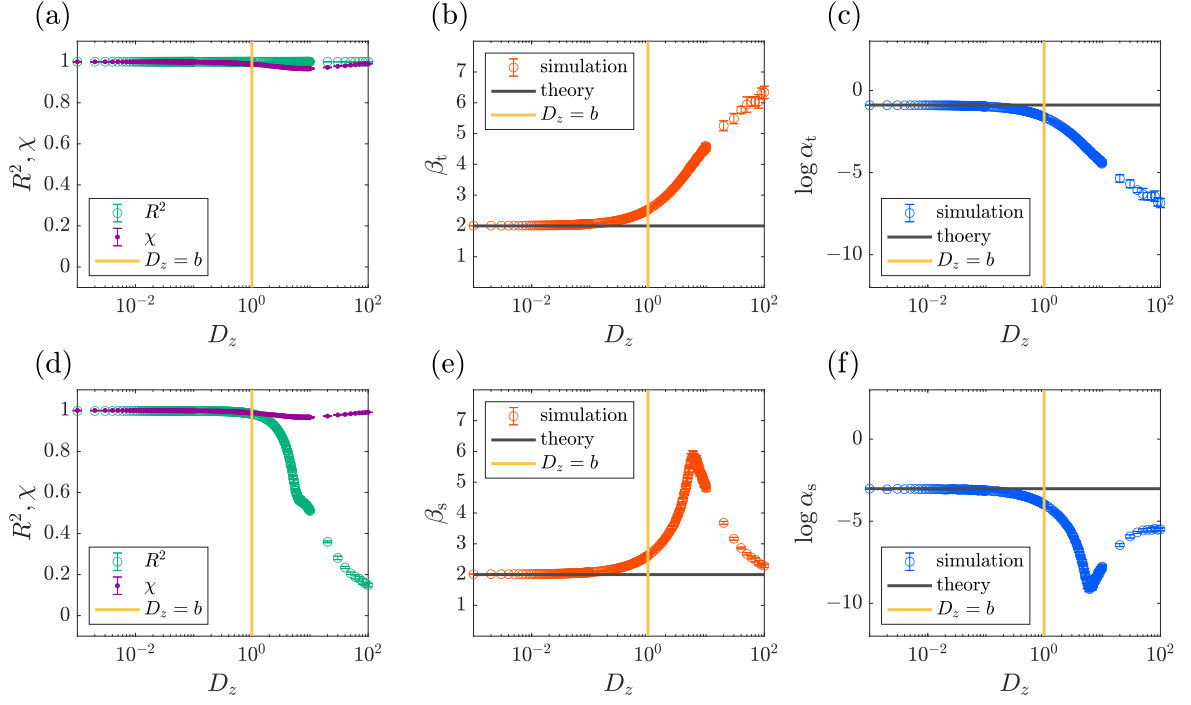


FIG. 7. Dependence of TL parameters on D_z in the coupled hyperchaotic Lorenz system. $a = 1, c = 0, k = 1, l = 1$ and $D_x = 1000, D_y = D_w = 0$. $N = 100, \sigma = 10, b = 8/3$, and ρ_i is randomly selected from a uniform distribution between 26.5 and 29.5. (a) R^2 of temporal TL. (b) Exponents of temporal TL. (c) Intercepts of temporal TL. (d) R^2 of spatial TL. (e) Exponents of spatial TL. (f) Intercepts of spatial TL.

- B. Z. Webb, Taylor's law for exponentially growing local populations linked by migration, *Theor. Popul. Biol.* **154**, 118–125 (2023).
- [42] A. Pikovsky, M. Rosenblum, and J. Kurths, *Synchronization: A Universal Concept in Nonlinear Sciences* (Cambridge University Press, 2002).

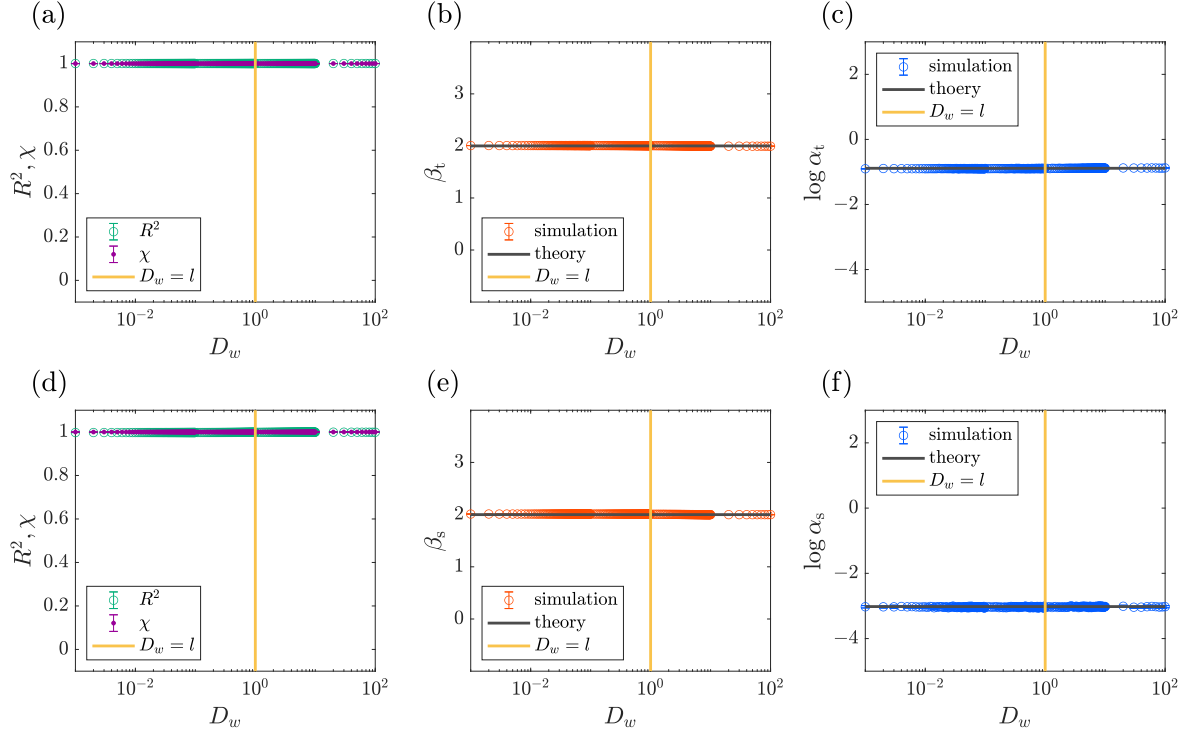


FIG. 8. Dependence of TL parameters on D_w in the coupled hyperchaotic Lorenz system. $a = 1, c = 0, k = 1, l = 1$ and $D_x = 1000, D_y = D_z = 0$. $N = 100, \sigma = 10, b = 8/3$, and ρ_i is randomly selected from a uniform distribution between 26.5 and 29.5. (a) R^2 of temporal TL. (b) Exponents of temporal TL. (c) Intercepts of temporal TL. (d) R^2 of spatial TL. (e) Exponents of spatial TL. (f) Intercepts of spatial TL.